Biotransformation of struvite by Aspergillus niger

Suyamud, Bongkotrat; Ferrier, John; Csetenyi, Laszlo; Inthorn, Duangrat; Gadd, Geoffrey Michael

Published in:
Environmental Microbiology

DOI:
10.1111/1462-2920.14949

Publication date:
2020

environmental microbiology

Environmental Microbiology (2020) **00**(00), 00–00 doi:10.1111/1462-2920.14949

Biotransformation of struvite by *Aspergillus niger*: phosphate release and magnesium biomineralization as glushinskite

Bongkotrat Suyamud,[1,2] John Ferrier,[2] Laszlo Csetenyi,[3] Duangrat Inthorn[4,5] and Geoffrey Michael Gadd [2,6*]

[1]*Department of Sanitary Engineering, Faculty of Public Health, Mahidol University, Bangkok, 10400, Thailand.*

[2]*Geomicrobiology Group, School of Life Sciences, University of Dundee, Dundee, DD1 5EH, Scotland, UK.*

[3]*Concrete Technology Group, Department of Civil Engineering, University of Dundee, Dundee, DD1 4HN, Scotland, UK.*

[4]*Department of Environmental Health Sciences, Faculty of Public Health, Mahidol University, Bangkok, 10400, Thailand.*

[5]*Center of Excellence on Environmental Health and Toxicology (EHT), Commission on Higher Education (CHE), Ministry of Education, Bangkok, 10210, Thailand.*

[6]*State Key Laboratory of Heavy Oil Processing, Beijing Key Laboratory of Oil and Gas Pollution Control, College of Chemical Engineering and Environment, China University of Petroleum, 18 Fuxue Road, Changping District, Beijing, 102249, China.*

Summary

Struvite (magnesium ammonium phosphate-$MgNH_4PO_4{\cdot}6H_2O$), which can extensively crystallize in wastewater treatments, is a potential source of N and P as fertilizer, as well as a means of P conservation. However, little is known of microbial interactions with struvite which would result in element release. In this work, the geoactive fungus *Aspergillus niger* was investigated for struvite transformation on solid and in liquid media. *Aspergillus niger* was capable of solubilizing natural (fragments and powder) and synthetic struvite when incorporated into solid medium, with accompanying acidification of the media, and extensive precipitation of magnesium oxalate dihydrate (glushinskite, $Mg(C_2O_4).2H_2O$) occurring under growing colonies. In liquid media, *A. niger* was able to solubilize natural and synthetic struvite releasing mobile phosphate (PO_4^{3-}) and magnesium (Mg^{2+}), the latter reacting with excreted oxalate resulting in precipitation of magnesium oxalate dihydrate which also accumulated within the mycelial pellets. Struvite was also found to influence the morphology of *A. niger* mycelial pellets. These findings contribute further understanding of struvite solubilization, element release and secondary oxalate formation, relevant to the biogeochemical cycling of phosphate minerals, and further directions utilizing these mechanisms in environmental biotechnologies such as element biorecovery and biofertilizer applications.

Introduction

The most important elements in struvite (magnesium ammonium phosphate-$MgNH_4PO_4{\cdot}6H_2O$) are phosphorus (P), nitrogen (N) and magnesium (Mg) (Tansel *et al*., 2018; Li *et al*., 2019) that are essential elements for all living organisms. P and Mg are well known for their involvement in ATP and nucleotide synthesis, ATP molecule normally occurring as a chelate with the Mg (Romani, 2013). Phosphorus is extremely important and, in phosphate, is widely used as a fertilizer, playing key roles in plant growth and development. It is the world's second largest nutritional supplement for crops after nitrogen (Adnan *et al*., 2017). Mg and its compounds are widely used in a number of high-value industrial applications such as in the production of certain alloys and catalysts, and in the chemical, electronic, pharmaceutical and agricultural industries (Tran *et al*., 2013; Tran *et al*., 2016; Kong *et al*., 2017).

In nature, struvite is formed through a variety of reactions with sources such as bird droppings and fish bones, and in humans may occur in urinary tract infections as kidney stones. In water treatment plants, it can extensively crystallize and accumulate in wastewater pipes (Le Corre *et al*., 2009). Because of this, control of struvite deposition has been widely investigated to reduce such pipeline blockages and adverse effects on the efficiency

Received 18 December, 2019; revised 6 February, 2020; accepted 18 February, 2020. *For For correspondence. E-mail g.m.gadd@dundee.ac.uk; Tel.: +44 1382 384767

of water and sewage systems (Le Corre *et al*., 2009). Struvite crystallization has also been investigated as a means for recovery of phosphorus, which can prevent eutrophication of surface waters and also provide a valuable fertilizer resource. Concern over P recovery is increasing because of its agricultural and industrial importance and the accelerating depletion of natural resources (Tao *et al*., 2016). The use of struvite as a plant fertilizer could improve nutrient acquisition, mitigate the loss of a potential P resource, and support plant productivity in a sustainable manner (Zhang *et al*., 2018; Li *et al*., 2019). One economic feasibility analysis, which took environmental benefits into account, concluded that phosphorus recovery, e.g. as struvite, is viable not only from sustainable development but also from an economic point of view (Molinos-Senante *et al*., 2011; Mayer *et al*., 2016). This may reduce P costs to farmers, possibly more so in developing countries where costs of mined P are higher (Mayer *et al*., 2016). However, there is a lack of research on the use of recovered struvite in contexts other than fertilizer applications, and little knowledge of the interactions of struvite with the soil microbiota, including mechanisms of dissolution (Talboys *et al*., 2016), which play such an important role in P mobilization from insoluble sources.

It is known that the geoactive soil fungus, *Aspergillus niger*, can transform insoluble metal compounds and minerals into soluble forms, a process of environmental significance in element cycling, plant productivity, and environmental biotechnology, e.g. metal bioleaching, biorecovery and bioremediation (Sayer and Gadd, 1997; Gadd *et al*., 2014; Ferrier *et al*., 2019). The ability of *A. niger* to colonize, penetrate, solubilize and/or precipitate minerals has been widely demonstrated, e.g. manganese oxides (Wei *et al*., 2012; Ferrier *et al*., 2019), rare earth-containing monazite sand and lanthanum compounds (Liang and Gadd, 2017; Kang *et al*., 2019), uranium and phosphorus-containing minerals (Liang *et al*., 2015) and metals (Al, Ti, Fe) in red mud (Vakilchap *et al*., 2016). These transformations largely depend on the excretion of various metabolites, particularly H^+ and organic acids, e.g. oxalic and citric acid (Gadd, 1999, 2007; Gadd *et al*., 2014). Oxalic acid is of high importance in metal mobilization and/or immobilization due to the formation of metal-oxalate complexes and/or precipitation of insoluble metal oxalates ($M^{n+}(C_2O_4)_{n/2}.xH_2O$) depending on the metal and environmental conditions (Gadd *et al*., 2014). Most strains of *A. niger* have been widely reported as geoactive, and phosphate-solubilizing capability is superior to that of many other phosphate-solubilizing organisms (Zhang *et al*., 2018). Therefore, the ability of this fungus to transform P-, Mg- and N-containing struvite is a worthy topic of study with important environmental implications. This research attempts to provide new insights into struvite biotransformation mechanisms, particularly in relation to colonization and penetration, mineral dissolution, element release and secondary oxalate biomineralization, using *A. niger* ATCC 1015. Our findings also contribute to an understanding of the applied potential of geoactive fungi in element and nutrient biorecovery.

Table 1. Growth on and solubilization of natural and synthetic struvite by *Aspergillus niger*.

Struvite type	Concentration (%)	Growth ratio	Solubilization ratio
Natural	0.25	1.05^{ab}	1.10^{a}
	0.5	1.06^{ab}	1.04^{a}
	1	0.94^{a}	1.08^{a}
Synthetic	0.25	1.05^{ab}	1.04^{a}
	0.5	1.09^{b}	1.03^{a}
	1	0.94^{a}	1.08^{a}

Different lowercase letters in the same column indicate that the values are significantly different at $p < 0.05$, based on one-way analysis of variance.

Results

Growth on and solubilization of struvite by A. niger *ATCC 1015*

Aspergillus niger ATCC 1015 was able to grow on all the struvite concentrations tested, and the growth rate increased with increasing struvite concentration over the range 0.25%–1.0% (w/v) (Table 1). There was a slight reduction of the growth rate on 1.0% (w/v) natural and synthetic struvite (Table 1). The growth rate of *A. niger* on 1.0% (w/v) natural and synthetic struvite was 14.6 ± 3.2 mm day^{-1} which was slightly lower than the control. The control growth rate of *A. niger* was 15.74 ± 0.28 mm day^{-1}. *Aspergillus niger* was also able to solubilize both natural and synthetic struvite, producing a clear solubilization halo in the agar surrounding and underneath the colony depending on the struvite concentration (Fig. 1A–C). Solubilization rates were not significantly different ($p < 0.05$) for both natural and synthetic struvite at all concentrations. Solubilization ratios were > 1.0, indicating an increased solubilization rate in relation to extension of the fungal hyphae (Sayer *et al*., 1995; Gharieb *et al*., 1998), especially evident at the lower struvite concentration of 0.25% (w/v). Such observations clearly showed the capacity of *A. niger* to solubilize the insoluble phosphate-containing mineral. After growth of *A. niger*, final media pH values were markedly decreased from the initial pH after 7 days of incubation. The initial pH values of control and struvite-containing media were pH 5.32 ± 0.01 and pH 7.03 ± 0.01, respectively. The production of acidity by *A. niger* was independent of the presence of struvite (Table 2) and similar pH profiles occurred for *A. niger*

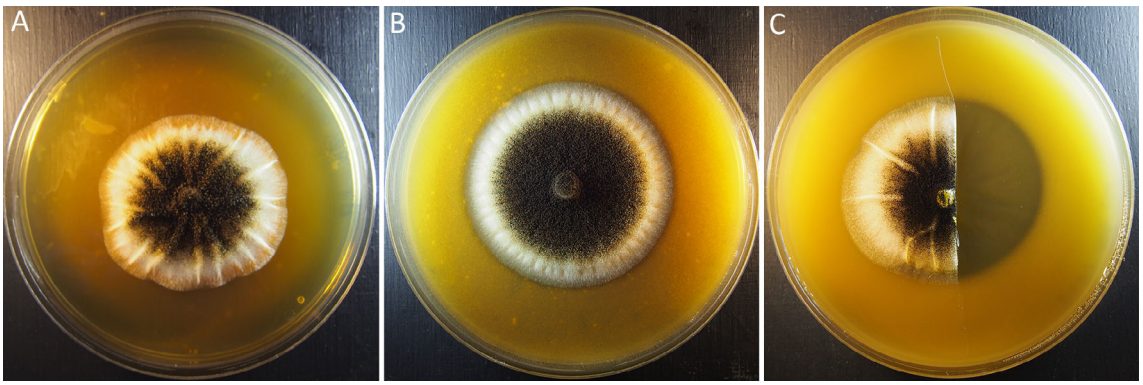

Fig. 1. Solubilization of struvite by *Aspergillus niger* in 9-cm diameter MEA plates. Colonies are shown after 3 days of incubation at 25°C in the dark. (A) MEA struvite-free control, (B) top view of colony on MEA containing 0.5% (w/v) natural struvite and (C) top view of MEA containing 1.0% (w/v) synthetic struvite with half of the colony and agar overlaying cellophane membrane removed to show the solubilization zone underneath the colony. Typical images are shown.

Table 2. Surface pH values of agar underneath growing *Aspergillus niger* colonies on control and struvite-containing medium.

	Struvite (%)	Initial pH	pH after 7 days	Biomass yield (g dry wt)
Control	0	5.32 ± 0.01^{a}	3.31 ± 0.05^{a}	0.35 ± 0.04^{a}
Natural struvite	0.25	6.83 ± 0.02^{b}	3.47 ± 0.16^{ab}	0.39 ± 0.03^{a}
	0.5	7.04 ± 0.02^{c}	3.73 ± 0.40^{ab}	0.33 ± 0.009^{a}
	1	7.06 ± 0.01^{cd}	3.37 ± 0.10^{a}	0.27 ± 0.01^{a}
Synthetic struvite	0.25	7.08 ± 0.01^{cd}	4.38 ± 0.16^{b}	0.32 ± 0.01^{a}
	0.5	7.11 ± 0.01^{d}	3.44 ± 0.26^{a}	0.31 ± 0.05^{a}
	1	7.06 ± 0.01^{cd}	4.09 ± 0.45^{ab}	0.29 ± 0.05^{a}

The pH was measured before and after 7 days growth at 25°C. The biomass yield was determined after 7 days. Data are given as means ± SD from three independent replicates. Different lowercase letters in the same column indicate that the values are significantly different at $p < 0.05$, based on one-way analysis of variance.

grown on natural or synthetic struvite. There was no significant difference in biomass yield between the control and struvite treatments (Table 2).

Direct interactions between Aspergillus niger *and fragments of natural struvite*

Small fragments of natural struvite (size 1–4 mm) were incubated with *A. niger* on malt extract agar (MEA) agar plates at 25°C in the dark, collected at various time intervals, and examined by scanning electronic microscopy (SEM). The resulting images revealed extensive colonization of the struvite fragments (Fig. 2A). Branched hyphae of *A. niger* were observed growing through fissures and emerging from the interior of the struvite after 2 days of incubation (Fig. 2B). Additionally, there was evidence of pore formation (Fig. 2C) indicating that *A. niger* could colonize the fragment interior by tunnelling (Fig. 2C). Secondary mineral formation surrounded the regions of *A. niger* colonization after 2 days of incubation (Fig. 2D and E). Figure 2F shows *A. niger* hyphae apparently penetrating a struvite crystal. Symmetrical octahedral biominerals frequently occurred after 4 days of incubation, the dimensions of these being approximately 40 to 200 μm (Fig. 2G and H). Almost all the resulting mineral debris were composed of such octahedral biomineral structures, with smaller amorphous components. After 8 days of incubation, the struvite fragments were significantly decayed and spore production was evident proximal to colonization and solubilization areas (Fig. 2I).

Transformation of struvite by Aspergillus niger

Crystals formed under colonies of *A. niger* growing on MEA agar medium amended with natural and synthetic struvite (Fig. 3A and D). Both natural and synthetic struvite were almost completely transformed on MEA agar plates after 1 week of incubation. SEM revealed the morphology of the octahedral biogenic crystals that formed with both natural and synthetic struvite as well as smaller amorphous debris (Fig. 3B, C, E and F). The dimensions of these crystals were approximately 30 to 90 μm. Energy dispersive X-ray analysis (EDXA) showed that the large octahedral crystals contained magnesium, carbon, and oxygen as predominant elements (Fig. 4B and D). All the crystals that formed with both natural and synthetic

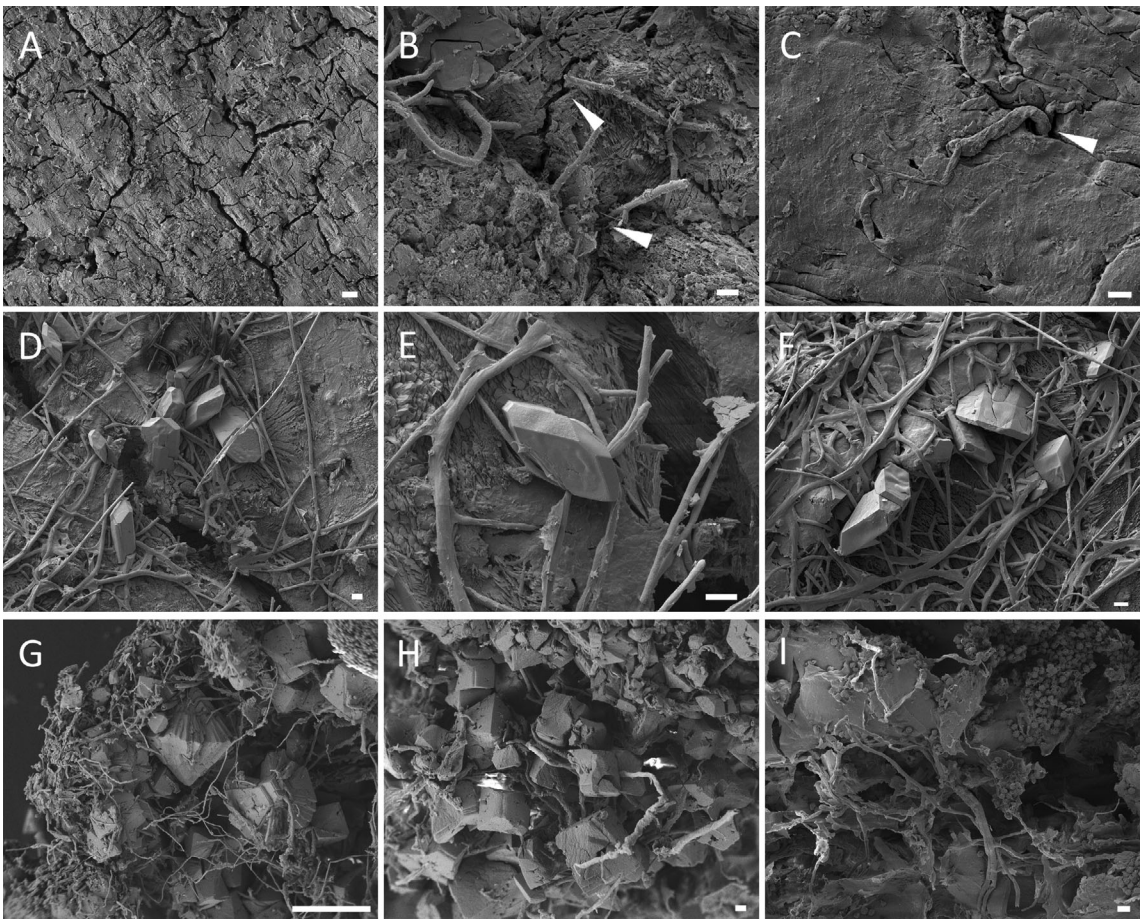

Fig. 2. SEM of direct interactions between natural struvite fragments (~1–4 mm) and *Aspergillus niger*.
A. Surface of control natural struvite. Scale bar = 10 μm.
B. Hyphae emerging from the interior of the struvite after 2 days of incubation at 25°C in the dark. Scale bar = 10 μm.
C. Fungal hypha tunneling on the surface of struvite after incubation with *Aspergillus niger* for 2 days at 25°C. Scale bar = 10 μm.
D and E. Secondary biomineral formation occurring around fungal colonization after 2 days of incubation at 25°C in the dark. Scale bars = 10 μm.
F. Fungal hyphae penetrating struvite after incubation for 2 days at 25°C. Scale bar = 10 μm.
G and H. Crystals produced by *A. niger* after 4 days of incubation with struvite. Scale bars: (G) 100 μm (H) 10 μm.
I. *Aspergillus niger* spores and bioweathered struvite fragments after growth for 8 days. Scale bar = 10 μm. Typical images are shown from several examinations.

struvite had approximately the same composition. Natural and synthetic struvite had similar elemental compositions consisting of magnesium, phosphorus and oxygen; a small amount of calcium was detected in natural struvite (Fig. 4A and C). X-ray diffraction (XRD) analysis of the biominerals collected from MEA plates containing 1.0% (w/v) natural or synthetic struvite after growth of *A. niger* for 1 week showed a clear match to reference patterns for Mg-oxalate dihydrate (glushinskite) (Fig. 5).

Struvite interactions with Aspergillus niger *in liquid media*

In liquid media, addition of both natural and synthetic struvite powder initially resulted in a white turbid suspension. However, clarification of the media occurred over the course of incubation with *A. niger*. Measurement of phosphate release showed that both the natural and synthetic struvite were completely solubilized by *A. niger* after 14 days of incubation (Fig. 6A and B). Phosphate release from natural struvite incubated with *A. niger* showed the highest values of 40.69 ± 1.13 mM after 12 days of incubation (Fig. 6A), whereas from synthetic struvite, released phosphate was 63.86 ± 0.48 mM after 8 days of incubation (Fig. 6B). The total phosphate concentration in natural and synthetic struvite was 3.82 ± 0.5 and 5.70 ± 0.77 mmol g dry wt^{-1} respectively. For both natural and synthetic struvite, abiotic control conditions showed only a small amount of phosphate release. Phosphate also occurred as a component in AP1-modified medium in the absence of struvite. The initial pH of AP1-modified medium before the addition of natural and synthetic struvite was approximately pH 4.6. After the addition of struvite, the pH rose to

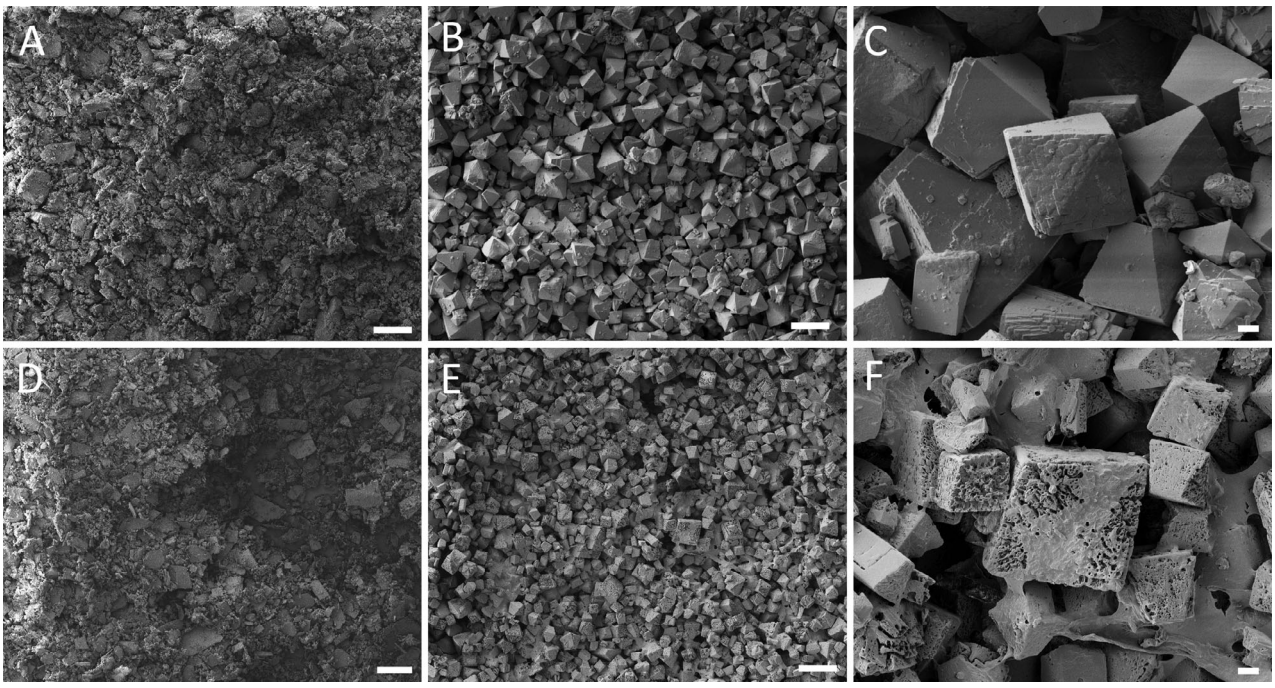

Fig. 3. SEM and light microscopy of mycogenic crystals produced on natural and synthetic struvite-amended MEA after fungal growth.
A. Natural struvite control. Scale bar = 100 μm.
B. Biomineral produced by *Aspergillus niger* on natural struvite amended agar after 7 days of incubation at 25°C. Scale bar = 100 μm.
C. Biomineral produced by *A. niger* on natural struvite amended agar after 7 days of incubation at 25°C. Scale bar = 10 μm.
D. Synthetic struvite control. Scale bar = 10 μm.
E. Biomineral produced by *A. niger* on synthetic struvite amended agar after 7 days of incubation at 25°C. Scale bar = 100 μm.
F. Biomineral produced by *A. niger* on synthetic struvite amended agar after 7 days of incubation at 25°C. Scale bar = 10 μm.
Typical images are shown from several examinations.

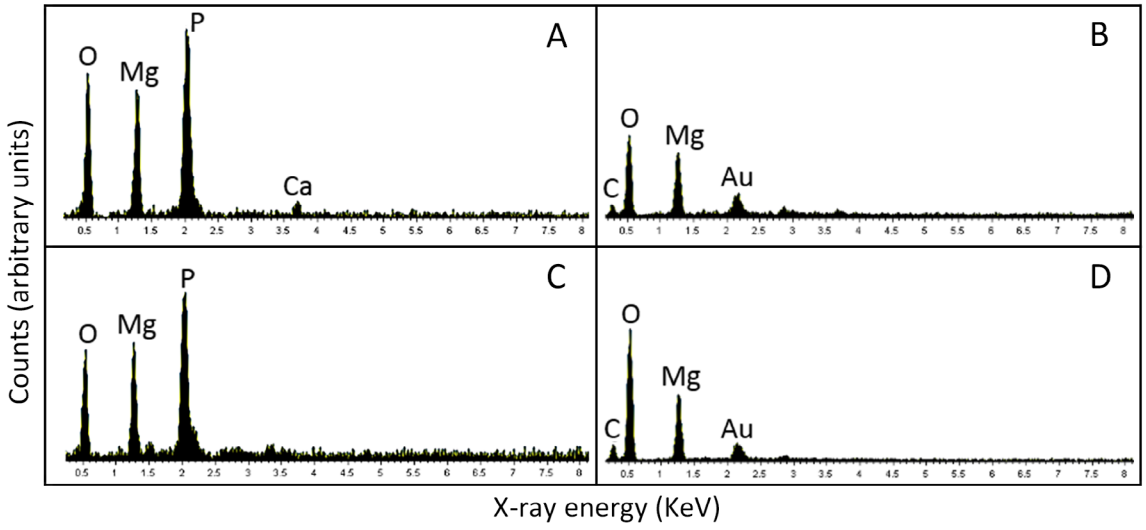

Fig. 4. EDXA of mycogenic crystals produced by *Aspergillus niger* during growth in the presence of natural and synthetic struvite for 7 days at 25°C in the dark.
A. Natural struvite control.
B. Mg-containing biomineral produced by *A. niger* during growth on natural struvite.
C. Synthetic struvite control.
D. Mg-containing biomineral produced by *A. niger* during growth on synthetic struvite. Typical spectra are shown from one of at least three determinations.

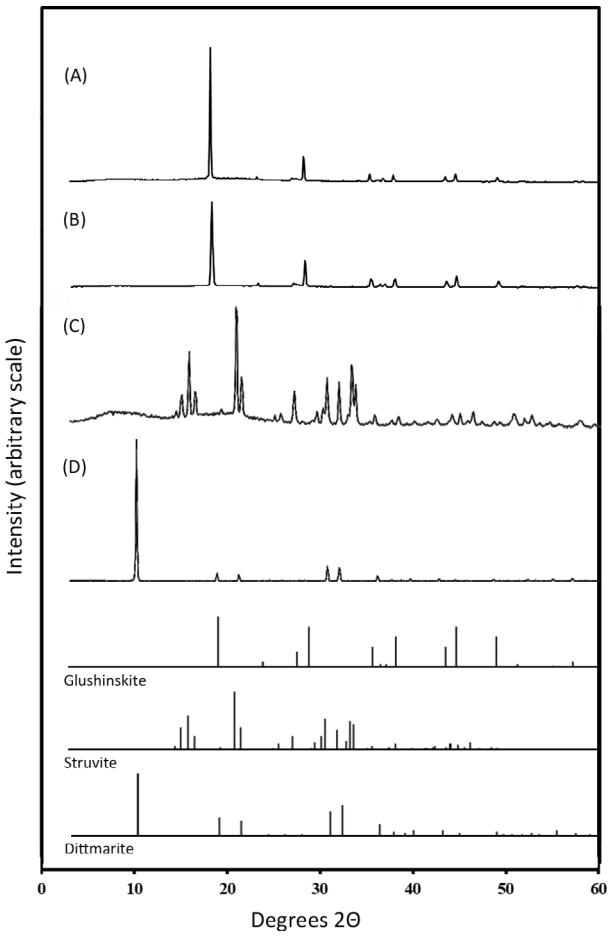

Fig. 5. X-ray powder diffraction (XRPD) patterns of crystals extracted from struvite-amended medium. Diffraction patterns were collected from crystals harvested from struvite-amended MEA medium after growth of *Aspergillus niger* for 7 days at 25°C in the dark.
(A) Transformed natural struvite, (B) transformed synthetic struvite, (C) natural struvite control and (D) synthetic struvite control. Both (A) and (B) contain Mg-oxalate dihydrate. The powder diffraction file reference patterns are (A) 26-1223 or 28-625 (Mg-oxalate dihydrate), (B) 28-625 (Mg-oxalate dihydrate), (C) 15-762 (struvite) and (D) 20-663 (dittmarite). Typical patterns are shown from one of at least three determinations.

pH 7.09 $\pm$ 0.15 for natural struvite (Fig. 6C) and pH 7.07 $\pm$ 0.2 for synthetic struvite (Fig. 6D). Over the first week of incubation, *A. niger* culture medium showed a dramatic decrease in pH, and after 14 days the final pH values for natural and synthetic struvite were pH 2.57 $\pm$ 0.18 and pH 3.47 $\pm$ 0.01 respectively (Fig. 6C and D). *Aspergillus niger* media without added struvite showed similar trends of pH reduction.

The Mg concentration in biomass-free culture supernatants was determined by atomic absorption spectrophotometry for *A. niger* incubated with natural or synthetic struvite. The complete solubilization of struvite by *A. niger* resulted in the release of Mg into the medium (Fig. 6E and F). Mg release from natural struvite incubated with *A. niger* showed the highest concentrations of 42.43 $\pm$ 6.09 mM after 7 days of incubation (Fig. 6E), and from synthetic struvite this was 44.66 $\pm$ 8.17 mM after 8 days of incubation (Fig. 6F). After this time, the Mg concentration in the supernatant showed a decrease. Only small amounts of Mg were detected in the abiotic controls for both natural and synthetic struvite. Total Mg concentrations in natural and synthetic struvite were 4.91 $\pm$ 0.04 and 4.75 $\pm$ 0.01 mmol g dry wt^{-1} respectively.

The Mg content of *A. niger* mycelial pellets was also determined (Table 3). Mg accumulation in pellets formed with natural and synthetic struvite were 2.50 $\pm$ 0.94 and 3.29 $\pm$ 0.41 μmol mg dry weight^{-1} respectively. Mg accumulation values for *A. niger* pellets incubated with natural and synthetic struvite were not significantly different but were clearly greater than the struvite-free control (Table 3). EDXA showed the elemental composition of *A. niger* pellets following 14 days of incubation with struvite included carbon, oxygen, magnesium and phosphorus (Fig. 7B and C). Mg was not detectable in control *A. niger* powdered pellets (Fig. 7A). XRD analysis of powdered *A. niger* pellets revealed the presence of glushinskite (Mg-oxalate dihydrate) in *A. niger* biomass incubated with natural and synthetic struvite (Fig. 8A–C). There was also a very minor phase present, whewellite (calcium oxalate monohydrate), in the powdered pellets of *A. niger* incubated with natural struvite. The XRD patterns of the powdered pellets of *A. niger* incubated with natural and synthetic struvite markedly contrasted to those obtained from *A. niger* pellets grown without struvite (Fig. 8A).

Effect of struvite on fungal pellet morphology and biomass yield

Biomass yields for *A. niger* incubated with natural or synthetic struvite for 14 days were 2.65 $\pm$ 0.08 and 2.78 $\pm$ 0.25 g dry weight^{-1}, respectively (Table 3). The biomass dry weight of *A. niger* collected from natural or synthetic struvite-amended medium was significantly different when compared with control *A. niger* biomass. The biomass dry weight of control *A. niger* was 1.32 $\pm$ 0.05 g dry weight^{-1} after 14 days. Light microscopy of pellet cross sections (Fig. 9A–F) showed differences in morphology between *A. niger* incubated in AP1-modified liquid medium with or without struvite. Hyphal formation by *A. niger* was, however, similar in natural struvite- and synthetic struvite-amended medium. Control *A. niger* displayed a robust spherical pelleted form (Fig. 9A, D and G). However, *A. niger* biomass collected from natural and synthetic struvite amended AP1-modified liquid medium showed swollen hyphal branches and aggregates (Fig. 9B, C, G–I) with the pellet core region exhibiting roughness with hair-like hyphae (Fig. 9E and F).

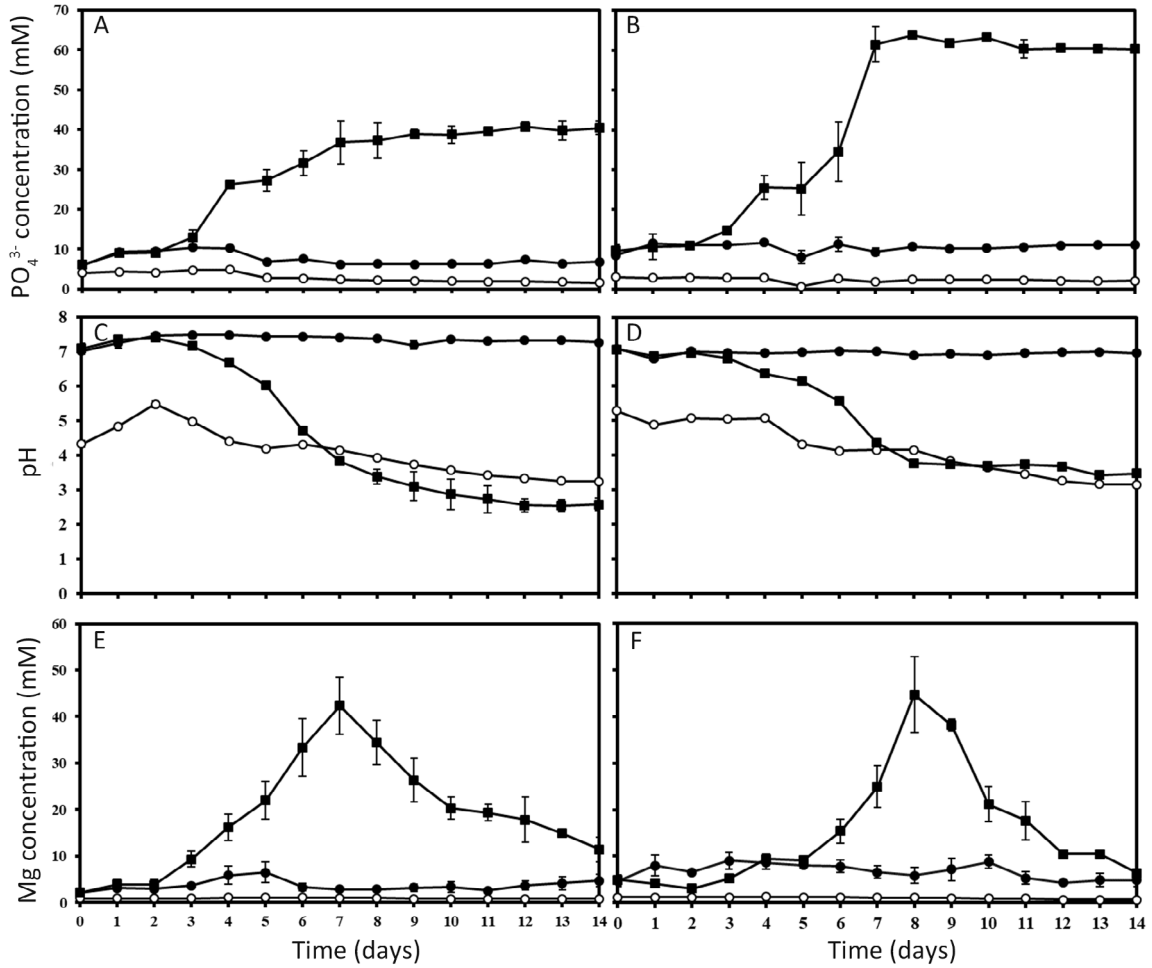

Fig. 6. (A, B) Phosphate (PO_4^{3-}) release, (C, D) changes in pH, and (E, F) magnesium (Mg) release during growth of *Aspergillus niger* in struvite-amended AP1 liquid medium for 14 days at 25°C. (A, C, E) *Aspergillus niger* with natural struvite and (B, D, F) with synthetic struvite. Solid square: *Aspergillus niger* incubated with struvite; open circle: *A. niger* struvite-free control; solid circle: abiotic struvite control. Data are averages of at least three replicates with error bars indicating the mean ± SD.

SEM also revealed that biogenic crystals associated with extracellular polymeric substances occurred within *A. niger* pellets (Fig. 9J–L).

Discussion

Struvite formation can be regarded as a form of phosphorus (P) conservation, where soluble P is converted from a waste resource into a solid P- and N-containing product of enhanced value (Kataki *et al*., 2016). Due to significant P loss, especially in water treatment, struvite utilization has become an important consideration since struvite crystallization could mitigate P loss and the recovered precipitate could be used as a biofertilizer or raw material in the chemical industry (Li *et al*., 2019). However, several current strategies for struvite precipitation, e.g. addition of alkali, Fe/Al salts or chemical inhibitors, can create some environmental safety issues (Kataki *et al*., 2016). Some biological strategies using bacteria and fungi have received attention for struvite biomineralization and biorecovery. For example, the halophilic marine actinomycete, *Mycobacterium marinum* sp. nov. H207 (Zhao *et al*., 2019), *Shewanella oneidensis* MR-1 (Luo *et al*., 2018) and an *Enterobacter* sp. EMB19 (Sinha *et al*., 2014) all could mediate struvite biomineralization for the recovery of phosphorus. Despite this, there are few real current applications of struvite and, surprisingly, little attention has been given to microbial interactions which can result in solubilization and release of the component elements which would be important in any biofertilizer applications. Therefore, understanding of some fundamental aspects of microbial struvite biotransformation is particularly well suited to inform future directions in struvite research and applications.

In this work, the ability of the ubiquitous geoactive soil fungus, *A. niger*, to colonize, solubilize and transform natural and synthetic struvite was clearly demonstrated.

Table 3. Biomass dry weight and Mg accumulation in biomass of *Aspergillus niger* pellets after 14 days growth at 25°C in liquid AP1 media without or supplemented with 1.0% (w/v) natural or synthetic struvite.

	Biomass (g dry weight)	Mg concentration (μmol.mg dry weight^{-1})
Struvite-free control	1.32 ± 0.05[a]	0.09 ± 0.006[a]
Natural struvite	2.65 ± 0.08[b]	2.50 ± 0.94[b]
Synthetic struvite	2.78 ± 0.25[b]	3.29 ± 0.41[b]

Data are given as means ± SD from three independent replicates. Different lowercase letters in the same column indicate that the values are significantly different at $p < 0.05$ based on one-way analysis of variance.

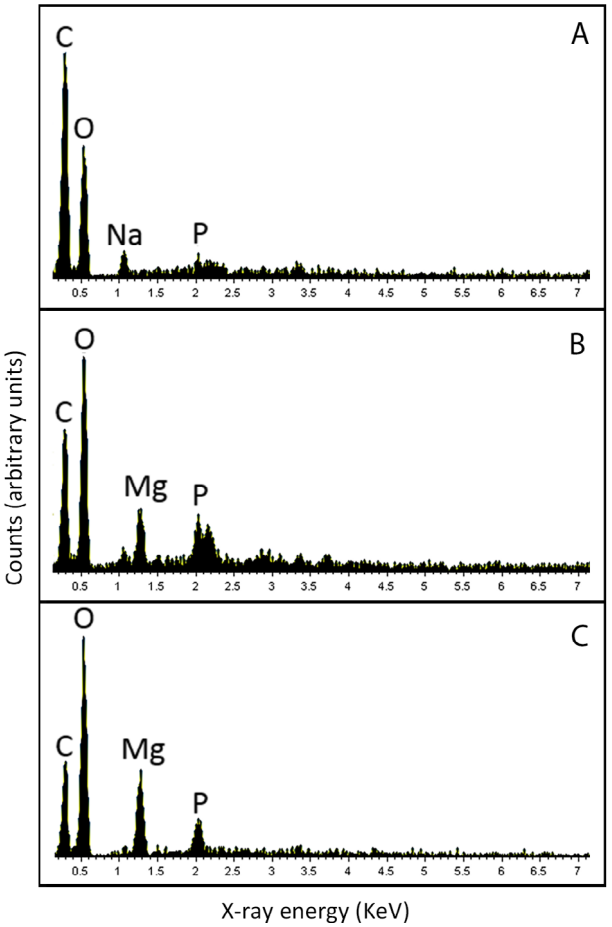

Fig. 7. EDXA of powdered mycelial pellets of *Aspergillus niger* after growth in liquid medium with natural or synthetic struvite.
A. *Aspergillus niger* struvite-free control.
B. *Aspergillus niger* after growth with natural struvite or (C) synthetic struvite showing the presence of Mg. *Aspergillus niger* was grown for 14 days at 25°C in the dark. Typical spectra are shown from one of at least three determinations.

Growth of *A. niger* ATCC 1015 on solid agar medium containing various concentrations of struvite led to struvite solubilization and the formation of clear solubilization haloes. It is well known that fungal metabolic activities can influence metal speciation and mobility and such processes are integral components of environmental element cycling (Gadd, 1999, 2007). *Aspergillus niger* has a well-established capacity for organic acid production, and oxalic acid is a commonly excreted metabolite (Sayer *et al*., 1995; Gharieb *et al*., 1998; Gadd *et al*., 2014). In this work, there was a strong correlation between struvite solubilization and oxalate excretion, and the production of magnesium oxalate occurred in both solid and liquid media. Mineralogical analysis of the biominerals formed confirmed the presence of magnesium oxalate dihydrate (glushinskite, $Mg(C_2O_4)\cdot 2H_2O$). Fungi can solubilize minerals by several mechanisms including (i) protonation (acidification), (ii) chelation (complexation) and (iii) metal accumulation by the biomass (Fomina *et al*., 2007; Gadd, 2007, 2010). Organic acids can provide protons for acidolysis and the acid anions can form complexes with metals leading to mineral dissolution (Gadd, 1999; Fomina *et al*., 2007). For example, lead complexation by fungal-derived oxalic acid was much more efficient for pyromorphite dissolution than acidification (Fomina *et al*., 2005), Citrate as a complexing agent can increase uranium mobilization (Ebbs *et al*., 1998), and oxalic acid produced by *A. niger* can transform insoluble manganese oxide minerals into manganese oxalate dihydrate (Wei *et al*., 2012). Struvite consists of PO_4^{3-} (tetrahedral), $Mg(6H_2O)^{2+}$ (octahedral) and NH_4^+ (tetrahedral) (Tansel *et al*., 2018). The transformation of struvite through the formation of glushinskite can be described by the following equation: $Mg^{2+} + 2C_2O_4^{2-} \rightarrow Mg(C_2O_4)_2$. Mg^{2+} can also form a bidentate complex with oxalate $(C_2O_4)^{2-}$ giving a complex anion ($Mg(C_2O_4)_2^{2-}$) which forms octahedral six-coordinate complexes. Mg oxalate dihydrate has a solubility product of 8.57×10^{-5} and is of higher solubility in water than several other metal oxalates, e.g. Ca, Sr, Ba and Cr (Gadd, 1999; Gadd *et al*., 2014). The tunnels that were observed within the struvite fragments can been explained as a result of colonization and dissolution within the mineral matrix (Jongmans *et al*., 1997; Soare *et al*., 2006; Fomina *et al*., 2010; Gadd *et al*., 2014) and also possible secondary precipitation around the biomass (Fomina *et al*., 2010).

In liquid media, struvite was completely solubilized releasing Mg^{2+}, NH_4^+, and PO_4^{3-} which demonstrates that pH as well as metal complexation is also a vital factor which leads to a free phosphate-rich supernatant. Many fungi, including *A. niger*, are well known for lowering the pH of their surrounding environment (Burford *et al*., 2003; Fomina *et al*., 2005; Boswell et al., 2007; Gadd *et al*., 2012), and acidolysis was the prime mechanism for toxic metal mineral solubilization by various

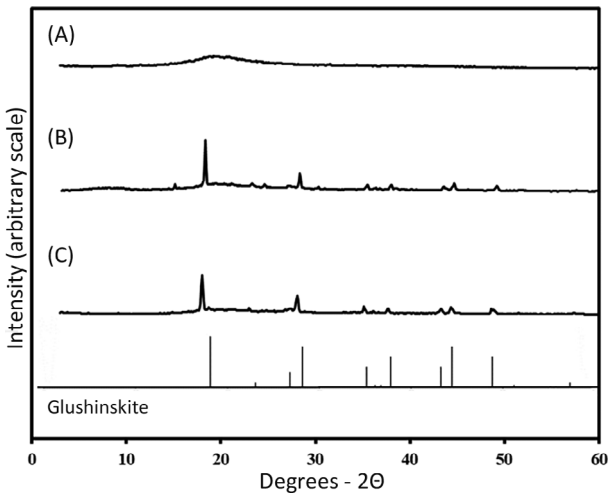

Fig. 8. X-ray powder diffraction patterns of powdered mycelial pellets of *A. niger* previously incubated in modified liquid AP1 media with natural or synthetic struvite.
(A) *Aspergillus niger* struvite-free control, (B) *A. niger* incubated with natural struvite and (C) *A. niger* incubated with synthetic struvite. Both (B) and (C) contain Mg-oxalate dihydrate. *Aspergillus niger* was grown for 14 days at 25°C in the dark. The powder diffraction file reference main phase is card 28-625, and also card 26-1223 (glushinskite, Mg-oxalate dihydrate). A minor phase is also present in *A. niger* incubated with natural struvite (20-231: whewellite, Ca-oxalate monohydrate). Typical patterns are shown from one of at least three determinations.

ericoid and ectomycorrhizal fungi (Fomina *et al*., 2004, 2005). The pH of both solid and liquid media decreased because of acidification by *A. niger*, and this is particularly evident with ammonium-containing media (Fomina *et al*., 2017). The amount of phosphate (PO_4^{3-}) released during the incubation period correlated with the decrease in pH for both natural and synthetic struvite. The relationship between pH and PO_4^{3-} release may depend on acidification and also organic acid production yields through the growth phase of *A. niger*. For example, white-rot basidiomycetes produce high concentrations of oxalate in the stationary phase, but lower concentrations during earlier active growth with little pH lowering of the medium pH (Gadd, 1999). This agrees with this study in that during the earlier stages of growth, high concentrations of PO_4^{3-} and Mg^{2+} were not found in culture supernatants. The reduction in Mg^{2+} concentration in the culture supernatant after 1 week of incubation was because of the precipitation of Mg^{2+} with oxalate.

Interestingly, both natural and synthetic struvite influenced *A. niger* biomass productivity and also affected pellet morphology and formation. In general, mycelial growth of *A. niger* under submerged conditions in liquid medium with agitation can comprise pellets arising from germination of spores and spore aggregates (Gow et al., 1999; Fomina and Gadd, 2002; Zhang and Zhang, 2016; Veiter *et al*., 2018). A wide range of factors such as the concentration of spore inoculum, pH and composition of growth medium, addition of anionic polymers (e.g. carbopol, polyacrylic acid) and genetic attributes of the particular fungal strain have all been implicated in pellet formation and structure (Fomina and Gadd, 2002). Depending on cultivation conditions, fungal species can exhibit different morphologies even for the same species (Gow et al., 1999; Veiter *et al*., 2018). In this study, addition of struvite into the liquid medium altered the initial pH which might have been one factor influencing pellet formation. At the initial steps in fungal development, electrostatic and hydrophobic interactions affect spore aggregation (Priegnitz *et al*., 2012; Zhang and Zhang, 2016; Veiter *et al*., 2018). For instance, conidia of *A. niger* are affected by surface charge (Grimm *et al*., 2004), and the electrostatic surface potential was affected by pH-dependent release of melanin leading to an irreversible reduction of the outermost layer between the spores and surrounding solution (Wargenau and Kwade, 2010). It was found that the pellets consisted of three main layers: a central core, with densely packed mycelium; a middle layer with looser mycelium; and an outer region, with loose hyphae. The presence of natural or synthetic struvite in the medium led to the appearance of numerous swollen hyphae in the outer region of *A. niger* pellets. However, dense pellets with compact hyphae occurred in the control medium. One of the main characteristics of fungal pellets is structural heterogeneity. Main causes of heterogeneity include limitation of both nutrients and oxygen which can result from dense hyphal packing in the pellet (Fomina and Gadd, 2002). The extent of limitation depends on the density of packing. In compact pellets, biomass production will terminate close to the surface and autolysis will occur. In less dense pellets, the actively growing shell of hyphae is wider, with substrates diffusing or flowing freely throughout the pellet (Schugerl *et al*., 1983; Wittler *et al*., 1986; Prosser and Tough, 1991; Fomina and Gadd, 2002).

Recovered phosphorus sources, such as struvite, may act as substitute for more soluble P fertilizers and therefore contribute to the conservation of existing finite P reserves in the natural environment (Talboys *et al*., 2016). Because of insolubility, struvite is a slow release fertilizer, which can be applied at high rates, and is believed to provide efficiency savings and environmental benefits over conventional soluble P fertilizer treatments (Massey *et al*., 2009; Cabeza *et al*., 2011; Molinos-Senante *et al*., 2011; Talboys *et al*., 2016). It seems clear that phosphate-solubilizing microorganisms, both bacteria and fungi, would have an important role in struvite solubilization and P release together with plant root exudates. Phosphate-solubilizing organisms are widespread in the natural environment (Sayer *et al*., 1995; Di Simine *et al*., 1998), and fungi in particular are known for high

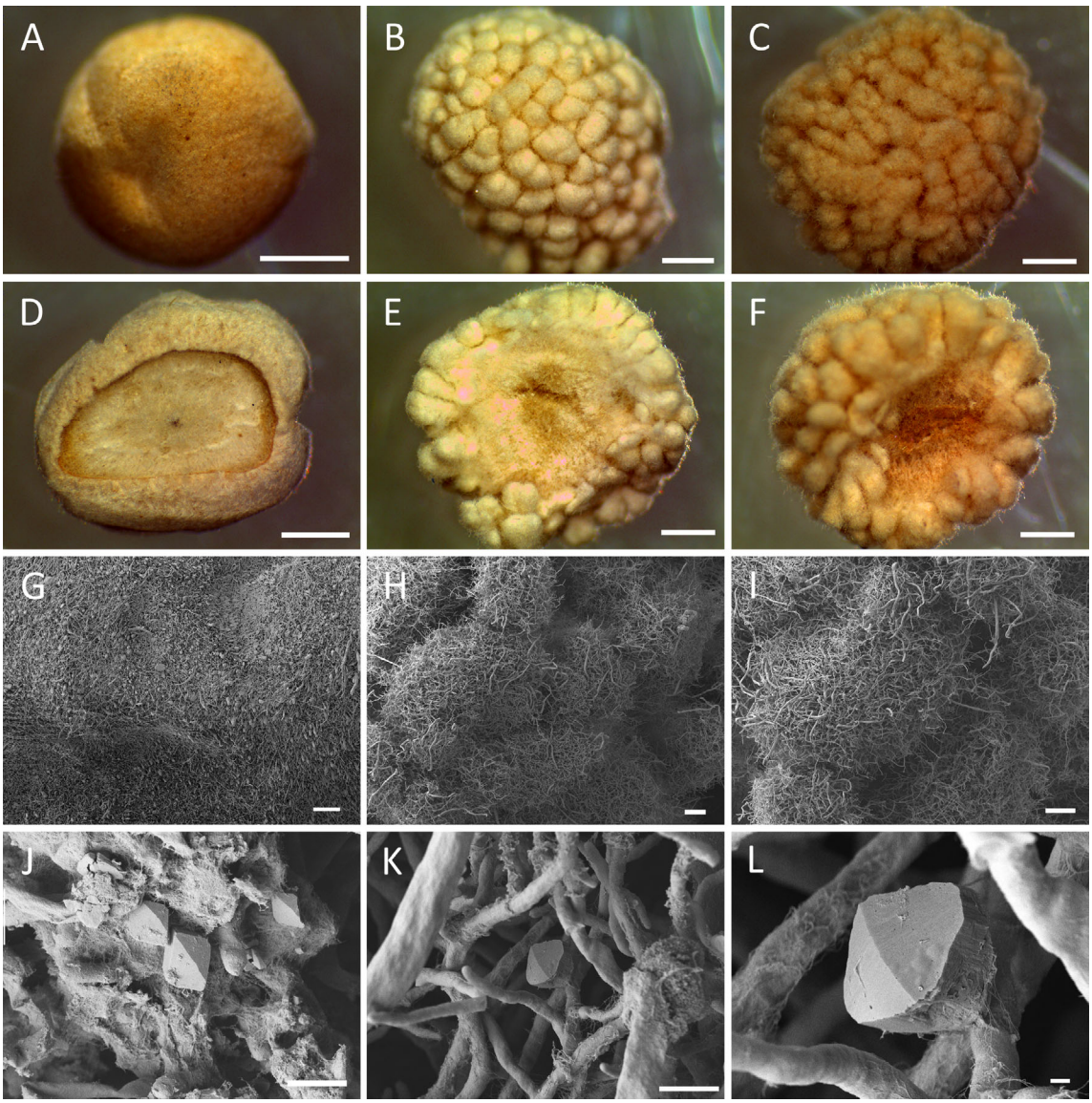

Fig. 9. Light microscopy and SEM images of *A. niger* pellets grown in liquid modified AP1 medium without or with 1.0% (w/v) natural and synthetic struvite and harvested after 14 days of incubation at 25°C with shaking at 125 rpm in the dark.
A, D and G. *Aspergillus niger* pellets collected from struvite-free control medium.
B, E and H. *Aspergillus niger* pellets collected from medium containing natural struvite.
C, F and I. *Aspergillus niger* pellets collected from medium containing synthetic struvite.
A, B and C. Cross section of *A. niger* pellets observed by light microscopy which show the outer surface of the fungal pellets.
D, E and F. Cross section of *A. niger* pellets observed by light microscopy which show the core region of the pellets.
G, H and I. SEM images of *A. niger* pellets showing differences in hyphal morphology when grown with and without struvite.
J, K and L. SEM images showing produced crystals bound by extracellular polysaccharide around hyphae. Scale bars = (A–F) 1 mm, (G–I) 100 μm, (J, K) 10 μm and (L) 1 μm. Typical images are shown from several examinations.

efficiencies in this regard through proton- and ligand-mediated dissolution, and to the benefit of plant growth (Sayer *et al*., 1997; Sayer and Gadd, 2001; Jacobs *et al*., 2002a, 2002b; Fomina *et al*., 2004, 2006; Xiao *et al*., 2008; Li *et al*., 2016; Zhang *et al*., 2018; Adhikari and Pandey, 2019). Efficient fungal P solubilizers occur in natural soils and have also been isolated from metal-polluted habitats, and the environs of phosphate mines (Sayer *et al*., 1995; Xiao *et al*., 2008; Li *et al*., 2016; Zhang *et al*., 2018). Organic acids are a key component of mineral dissolution mechanisms in fungi (Gadd, 1999, 2007; Gadd *et al*., 2014). Some work has suggested that struvite solubilization was better under acidic conditions, which would favour fungal populations (De Vries *et al*., 2017). In view of the ubiquity of phosphate-solubilizing microorganisms in soil, it seems unlikely that bioaugmentation of struvite

application with a phosphate-solubilizer, such as *A. niger* and thereby adding a further economic cost, would be necessary, although many studies have demonstrated the beneficial effects of plant inoculation with bacterial and fungal phosphate-solubilizing organisms (Whitelaw, 2000; Khan *et al*., 2010; Alori *et al*., 2017). Enhancement of struvite solubilization by bioaugmentation would also undermine the value of struvite as a slow P-release fertilizer (Talboys *et al*., 2016).

To summarize, our findings have provided further light on potential fungal roles in struvite solubilization, element release and biomineralization which may be important in fertilizer and other soil management applications, but are also of possible significance for other biotechnological purposes such as metal or element biorecovery through oxalate or phosphate bioprecipitation. Mg is a very important metal in technology and its numerous applications have led to increasing Mg metal production across the world (Tran *et al*., 2013; Tran *et al*., 2016). Mg-oxalate has also been used for the synthesis of nanoparticulate magnesium oxide. Mg oxide is important because it is used in catalysts, refractory materials, adsorbents, superconductors and ferroelectric materials (Mastuli *et al*., 2012). Secondly, the free phosphate rich supernatant provides a means of phosphate recovery and purification, as well as a reactive medium for metal biorecovery from solution as insoluble phosphates or oxalates (Liang and Gadd, 2017). In conclusion, this first demonstration of struvite transformation by a fungus extends understanding of struvite solubilization and biomineralization mechanisms, relevant to the biogeochemical cycling of phosphorus, and suggests further directions utilizing these mechanisms for applications in environmental biotechnology such as metal and element biorecovery.

Experimental procedures

Organisms and media

A wild-type *Aspergillus niger* van Tieghem (ATCC 1015) was maintained on MEA (Sigma-Aldrich, St. Louis, MO, USA) plates at 25°C in the dark for at least 3 days prior to experiments. No other strains were used, and throughout this paper *A. niger* refers to *A. niger* ATCC 1015. Modified AP1 medium includes (g L^{-1} Milli-Q water): D-glucose, 40 (Merck, Readington Township, NJ, USA), $NaNO_3$, 5 (Sigma-Aldrich), KH_2PO_4, 0.5 (Sigma-Aldrich), $MgSO_4{\cdot}7H_2O$, 0.2 (Sigma-Aldrich), NaCl, 0.1 (Sigma-Aldrich), $CaCl_2$, 0.05 (Sigma-Aldrich), $FeSO_4{\cdot}7H_2O$, 0.0025 (Sigma-Aldrich) and trace elements $ZnSO_4$, 0.04 (BDH, Poole, Dorset, UK), $MnSO_4$, 0.04 (Sigma-Aldrich) and $CuSO_4$, 0.004 (BDH, UK). Concentrated stock solutions of the mineral salts were made for all individual ingredients and autoclaved at 121°C for 15 min before being added to sterile 4%(w/v) glucose solution to the appropriate final concentrations and a final volume of 100 ml in a 250 ml Erlenmeyer flask.

Struvite preparation

Natural and synthetic struvite were used as the struvite source in solid and liquid media. Natural struvite (fragmented form of approximate diameters 1–4 mm and powdered forms of diameter 335 μm) was kindly obtained from Veolia Water Outsourcing (London, UK) from their operating site in Exeter, UK. Synthetic struvite was prepared by adding 3.038 g $MgCl_2$ (Sigma-Aldrich), 5.408 g NH_4Cl (Sigma-Aldrich) and 7.728 g K_2HPO_4 (BDH) to 1 L of Milli-Q water to obtain an equimolar Mg: N: P ratio. Then, 5 M NaOH was used to adjust the pH to 8.5 and stirred continuously using a magnetic stirrer for 5 min. Precipitated struvite was collected by filtration through Whatman filter paper and dried in a desiccator to constant weight at ambient temperature for at least 2 days. XRD analysis confirmed that the precipitate produced was the monohydrate form, dittmarite ($MgNH_4PO_4{\cdot}H_2O$).

Struvite solubilization

In solid media, MEA was used to support fungal growth in the absence (control) or presence of struvite. MEA without or containing 0.25%, 0.5% and 1.0% (w/v) struvite was used in 90 mm diameter Petri dishes. Prior to inoculation, 84 mm diameter discs of sterile cellophane membrane (Focus Packaging and Design, Louth, UK) were placed aseptically on the surface of the agar to provide a convenient of removing the mycelium. The plates were then inoculated using 5 mm diameter discs of mycelia cut from the leading edge of actively growing colonies using a sterile cork borer. Daily measurements were made of colony diameter and any clear solubilization zones present (Sayer *et al*., 1995). Measurements were discontinued when the colonies or clear zones had reached the edge of the Petri dish. Fungal biomass was removed from the agar by peeling from the cellophane membrane using a clean scalpel. The mycelia were dried to constant weight at 105°C for at least 2 days. Further to the above, the ability of *A. niger* to colonize, penetrate and transform struvite was also investigated using MEA agar. Small fragments of natural struvite (1–4 mm) were placed on MEA agar plates which were inoculated with an agar plug (diam. 5 mm) of *A. niger* and incubated at 25°C in the dark. Fragment samples were removed at selected time periods and examined using SEM, EDXA and XRD.

For struvite solubilization in liquid media, *A. niger* was inoculated on MEA slants and grown for 14 days at 25°C before use. To obtain a spore suspension, 30 ml of sterile

0.05% (v/v) Tween 80 was added to the slants and mixed well. The mycelial/spore suspension was then filtered through sterile 63 μm nylon mesh (John Staniar & Co., Manchester, UK) to remove mycelial fragments from the suspension. The spore solutions were centrifuged (2553*g*, 30 min), washed three times with sterile Milli-Q water to remove any remaining Tween 80 and resuspended as a concentrated solution in sterile Milli-Q water. The initial spore concentration in experimental flasks was 1×10^6 ml^{-1}. Modified AP1 liquid medium was used in these experiments with an initial pH of approximately pH 4.6 (see previously). Two hundred millilitres of modified AP1 medium in 500 ml Erlenmeyer flasks was supplemented with 1% (w/v) synthetic and natural struvite (particle diameter 335 μm) which had been previously oven-sterilized at 105°C for at least 2 days. The inoculated flasks were incubated in a rotary shaking incubator (Infors HT, Basel, Switzerland) at 105 rpm in the dark at 25°C for at least 2 weeks. Medium aliquots (2 ml) were collected daily, centrifuged (2553*g*, 30 min) and the supernatants used for measurement of pH, phosphate (PO_4^{3-}) and Mg concentrations. Fungal biomass was also collected after 2 weeks by paper filtration, suspended in 100 ml Milli-Q water and centrifuged (2553*g*, 30 min) to obtain the biomass dry weight and for determination of Mg accumulation.

Purification of biogenic crystals produced during growth of A. niger *on struvite-containing solid medium*

Crystals formed in the agar under fungal colonies and in the clear zones of solubilization when *A. niger* was grown in the presence of natural and synthetic struvite. The crystals were extracted by gently homogenizing the agar with Milli-Q water at 80°C in a crystallizing dish and, after settling, were washed at least three times with Milli-Q water. Crystals were dried to constant weight in a vacuum desiccator prior to examination by SEM, EDXA and XRD.

Measurement of inorganic phosphate (PO_4^{3-}) release

Biomass-free spent culture supernatants were analyzed for PO_4^{3-} release from the struvite using a modified molybdenum blue assay (He and Honeycutt, 2005). All reagents used for this reaction were prepared according to Dick and Tabatabai (1977). The total concentration of PO_4^{3-} in the struvite was measured by dissolving the natural or synthetic struvite in 1 M HCl. The reagent consisted of the following: Reagent A: 0.704 g of L-ascorbic acid (0.1 M) (Sigma-Aldrich) and 3.268 g of trichloroacetic acid (0.5 M) (Sigma-Aldrich) were dissolved in 10 ml Milli-Q water and the final volume adjusted to 40 ml; Reagent B: 2.472 g of ammonium molybdate (0.01 M) (Sigma-Aldrich) was dissolved in 100 ml Milli-Q water and the final volume was then adjusted to 200 ml; Reagent C: 5.882 g of sodium citrate (0.1 M) (Sigma-Aldrich) and 5.196 g of sodium arsenite (0.2 M) (Sigma-Aldrich) were dissolved in 100 ml Milli-Q water and then 10 ml of glacial acetic acid was added, the final volume being adjusted to 200 ml with Milli-Q water. Aliquots of biomass-free culture supernatants from *A. niger* culture media, incubated with or without struvite, were diluted to the appropriate concentration before testing. Then, 0.32 ml aliquots of diluted samples were collected in 1.5 ml Eppendorf tubes (Eppendorf, Hamburg, Germany). Standard curves were generated using a series of KH_2PO_4 solutions ranging from 1.5 to 25 $\mu g\ ml^{-1}$ KH_2PO_4. 0.40 μl reagent A, 0.08 ml reagent B and 0.20 ml reagent C were sequentially added to the samples. After the addition of each solution, samples were vortexed for 1 min using a Vortex Genie 2 (VWR, Radnor, USA). 500 μl samples were then transferred to 1 x 1 cm polystyrene cuvettes (Sarstedt, Nümbrecht, Germany), and the absorbance at 850 nm of the molybdenum blue was recorded using an Ultrospec 2100 Pro spectrophotometer (GE Healthcare, UK) after a 30 min reaction time. Measurement of the total phosphate concentration in the struvite samples was achieved after dissolving 1 g natural or synthetic struvite in 100 ml 1 M HCl.

pH measurement

The pH of liquid media, culture supernatants and agar surfaces before and after incubation with *A. niger* were measured using an Orion 920+ pH meter (Thermo Fisher Scientific, Loughborough, UK) equipped with a flat-tip electrode (VWR International, Lutterworth, UK).

Measurement of Mg accumulation

Biomass-free culture supernatants from each flask and acid-digested biomass extracts were analyzed for Mg concentration using an AAnalyst 400 atomic absorption spectrophotometer (PerkinElmer Instruments, Waltham, MA, USA) using appropriate lamps and standard solutions. Fungal biomass was collected by paper filtration, resuspended in 100 ml Milli-Q water and centrifuged (2553*g*, 30 min). Fungal biomass was dried at 105°C for several days until the weight was constant. Fifty milligrams of dry biomass were digested in 3 ml 16 M HNO_3 at 90°C until the solution became clear following the method of Li *et al*. (2014). The supernatant was then filtered using 0.2 μm pore size cellulose acetate membrane filters (Whatman International, Maidstone, England) and diluted to an appropriate concentration using 0.2 M

HNO_3. The total Mg concentration in struvite was measured after dissolving 1 g of natural or synthetic struvite in 100 ml^{-1} 1 M HCl, and measuring as above.

SEM, EDXA and XRD

Samples of biomass and struvite from solid and liquid media were fixed for ~24 h in 2.5% (v/v_{aq}) glutaraldehyde solution in 5 mM piperazine-N,N′-bis (2-ethanesulfonic acid) (PIPES) buffer adjusted to pH 6.5 with 1 M NaOH. Samples were washed twice with 5 mM PIPES buffer (pH 6.5) before dehydration using an ascending ethanol series [30%–100% (v/v_{aq})], with the samples being left for 10 min at each step. Samples were then dried using a BAL-TEC CPD 030 CO_2–critical point drier (Bal-Tec company, Los Angeles, CA, USA). Dried samples were mounted on aluminium stubs using carbon adhesive tape and stored in a desiccator at room temperature. Samples were coated with 10 nm gold and palladium using a Cressington 208HR sputter coater (Cressington Scientific Instruments, Watford, UK) and examined using a field emission scanning electron microscope (JEOL JSM-7400F) operating at an accelerating voltage of 5 kV for imaging and 20 kV for EDXA.

Mineralogical characterization by XRD was conducted using a Siemens D5000 powder X-ray diffractometer (Siemens Healthineers, Henkestraße 127, 91052 Erlangen, Germany). Samples were ground to a fine powder using a mortar and pestle before being applied to PVC slides. Diffraction patterns were recorded using angular increments of 0.1° 2Θ from 3°–60° 2Θ, at a rate of 1° 2Θ/min. A Cu-Kα source was used, operating at 40 mA and 40 kV, with a scintillation detector.

Light microscopy

A Leica EZ4 HD stereo microscope with LED illumination, a parfocal optical system and 60° viewing angle (Meyer Instruments, Houston, TX, USA) was used to examine *A. niger* pellet morphology after incubation with natural and synthetic struvite. The integrated 3.0 Mega-Pixel CMOS camera with Leica LAS EZ software (Meyer Instruments) was used to process images.

Statistical analysis

Statistical analyses were performed using the SPSS Statistics Package, version 22.0. Levene tests were conducted for assessing the normal distribution of the growth ratio, solubilization ratios, pH and biomass. Subsequently, one-way analysis of variance was performed followed by post hoc analysis, Tukey's honestly significant difference test.

Acknowledgements

This research was financially supported by Thailand Science Research and Innovation (TSRI) through the Royal Golden Jubilee PhD Program (grant number PHD/0177/2556). G.M.G. gratefully thanks the Natural Environment Research Council (NE/M010910/1 (TeaSe); NE/M011275/1 (COG^3)) for financial support of the Geomicrobiology Group. J.F. gratefully acknowledges receipt of a NERC PhD studentship as part of the COG^3 award. Thanks are also due to Dr. Yongchang Fan (School of Science and Engineering, University of Dundee) for assistance with EDXA and SEM.

References

Adhikari, P., and Pandey, A. (2019) Phosphate solubilization potential of endophytic fungi isolated from *Taxus wallichiana* Zucc. roots. *Rhizosphere* **9**: 2–9.

Adnan, M., Shah, Z., Fahad, S., Arif, M., Alam, M., Khan, I. A., *et al*. (2017) Phosphate-solubilizing bacteria nullify the antagonistic effect of soil calcification on bioavailability of phosphorus in alkaline soils. *Sci Rep* **7**: 16131.

Alori, E.T., Glick, B.R., and Babalola, O.O. (2017) Microbial phosphorus solubilization and its potential for use in sustainable agriculture. *Front Microbiol* **8**: 971.

Boswell, G.P., Jacobs, H., Ritz, K., Gadd, G.M., and Davidson, F.A. (2007) The development of fungal networks in complex environments. *Bull Math Biol* **69**: 605–634.

Burford, E.P., Fomina, M., and Gadd, G.M. (2003) Fungal involvement in bioweathering and biotransformation of rocks and minerals. *Mineral Mag* **67**: 1127–1155.

Cabeza, R., Steingrobe, B., Romer, W., and Claassen, N. (2011) Effectiveness of recycled P products as P fertilisers, as evaluated in pot experiments. *Nutr Cycl Agroecosyst* **91**: 173–184.

De Vries, S.C., Postma, R., Van Scholl, L., Blom-Zandstra, M., Verhagen, A. and Harms, I. (2017) Economic feasibility and climate benefits of using struvite from the Netherlands as a phosphate (P)fertilizer in West Africa. Wageningen Research, Report WPR-673, 48 pp., https://doi.org/10.18174/417821

Di Simine, C.D., Sayer, J.A., and Gadd, G.M. (1998) Solubilization of zinc phosphate by a strain of *Pseudomonas fluorescens* isolated from a forest soil. *Biol Fertil Soil* **28**: 87–94.

Dick, W.A., and Tabatabai, M.A. (1977) Determination of orthophosphate in aqueous solutions containing labile organic and inorganic phosphorus compounds. *J Environ Qual* **6**: 82–85.

Ebbs, S.D., Norvell, W.A., and Kochian, L.V. (1998) The effect of acidification and chelating agents on the solubilization of uranium from contaminated soil. *J Environ Qual* **27**: 1486–1494.

Ferrier, J., Yang, Y., Csetenyi, L., and Gadd, G.M. (2019) Colonization, penetration and transformation of manganese oxide nodules by *Aspergillus niger*. *Environ Microbiol* **21**: 1821–1832.

Fomina, M., and Gadd, G.M. (2002) Influence of clay minerals on the morphology of fungal pellets. *Mycol Res* **106**: 107–117.

Fomina, M.A., Alexander, I.J., Hillier, S., and Gadd, G.M. (2004) Zinc phosphate and pyromorphite solubilization by soil plant-symbiotic fungi. *Geomicrobiol J* **21**: 351–366.

Fomina, M.A., Alexander, I.J., Colpaert, J.V., and Gadd, G. M. (2005) Solubilization of toxic metal minerals and metal tolerance of mycorrhizal fungi. *Soil Biol Biochem* **37**: 851–866.

Fomina, M., Charnock, J.M., Hillier, S., Alexander, I.J., and Gadd, G.M. (2006) Zinc phosphate transformations by the *Paxillus involutus*/pine ectomycorrhizal association. *Microbial Ecol* **52**: 322–333.

Fomina, M., Charnock, J.M., Hillier, S., Alvarez, R., and Gadd, G.M. (2007) Fungal transformations of uranium oxides. *Environ Microbiol* **9**: 1696–1710.

Fomina, M., Burford, E.P., Hillier, S., Kierans, M., and Gadd, G.M. (2010) Rock-building fungi. *Geomicrobiol J* **27**: 624–629.

Fomina, M., Bowen, A.D., Charnock, J.M., Podgorsky, V.S., and Gadd, G.M. (2017) Biogeochemical spatio-temporal transformation of copper in *Aspergillus niger* colonies grown on malachite with different inorganic nitrogen sources. *Environ Microbiol* **19**: 1310–1321.

Gadd, G.M. (1999) Fungal production of citric and oxalic acid: importance in metal speciation, physiology and biogeochemical processes. *Adv Microb Physiol* **41**: 47–92.

Gadd, G.M. (2007) Geomycology: biogeochemical transformations of rocks, minerals, metals and radionuclides by fungi, bioweathering and bioremediation. *Mycol Res* **111**: 3–49.

Gadd, G.M. (2010) Metals, minerals and microbes: geomicrobiology and bioremediation. *Microbiol* **156**: 609–643.

Gadd, G.M., Rhee, Y.J., Stephenson, K., and Wei, Z. (2012) Geomycology: metals, actinides and biominerals. *Environ Microbiol Rep* **4**: 270–296.

Gadd, G.M., Bahri-Esfahani, J., Li, Q., Rhee, Y.J., Wei, Z., Fomina, M., and Liang, X. (2014) Oxalate production by fungi: significance in geomycology, biodeterioration and bioremediation. *Fungal Biol Rev* **28**: 36–55.

Gharieb, M.M., Sayer, J.A., and Gadd, G.M. (1998) Solubilization of natural gypsum ($CaSO_4.2H_2O$) and the formation of calcium oxalate by *Aspergillus niger* and Serpula himantioides. *Mycol Res* **102**: 825–830.

Gow, N.A.R., Robson, G.D., and Gadd, G.M. (1999) *The Fungal Colony*. Cambridge, UK: Cambridge University Press.

Grimm, L.H., Kelly, S., Hengstler, J., Gobel, A., Krull, R., and Hempel, D.C. (2004) Kinetic studies on the aggregation of *Aspergillus niger* conidia. *Biotechnol Bioeng* **87**: 213–218.

He, Z., and Honeycutt, C.W. (2005) A modified molybdenum blue method for orthophosphate determination suitable for investigating enzymatic hydrolysis of organic phosphates. *Comm Soil Sci Plant Anal* **36**: 1373–1383.

Jacobs, H., Boswell, G.P., Ritz, K., Davidson, F.A., and Gadd, G.M. (2002a) Solubilization of calcium phosphate as a consequence of carbon translocation by *Rhizoctonia solani*. *FEMS Microbiol Ecol* **40**: 65–71.

Jacobs, H., Boswell, G.P., Ritz, K., Davidson, F.A., and Gadd, G.M. (2002b) Solubilization of metal phosphates by *Rhizoctonia solani*. *Mycol Res* **106**: 1468–1479.

Jongmans, A.G., van Breemen, N., Lundström, U., Van Hees, P.A.W., Finlay, R.D., Srinivasan, M., *et al*. (1997) Rock-eating fungi. *Nature* **389**: 682–683.

Kang, X., Csetenyi, L., and Gadd, G.M. (2019) Biotransformation of lanthanum by *Aspergillus niger*. *Appl Microbiol Biotechnol* **103**: 981–993.

Kataki, S., West, H., Clarke, M., and Baruah, D.C. (2016) Phosphorus recovery as struvite: recent concerns for use of seed, alternative Mg source, nitrogen conservation and fertilizer potential. *Res Conserv Recycling* **107**: 142–156.

Khan, M.S., Zaidi, A., Ahemad, M., Oves, M., and Wani, P.A. (2010) Plant growth promotion by phosphate solubilizing fungi—current perspective. *Arch Agron Soil Sci* **56**: 73–98.

Kong, X., Chen, Z., Wu, Y., Wang, R., Chen, J., and Ding, L. (2017) Synthesis of Cu–Mg/ZnO catalysts and catalysis in dimethyl oxalate hydrogenation to ethylene glycol: enhanced catalytic behaviour in the presence of a Mg^{2+} dopant. *RSC Adv* **7**: 49548–49561.

Le Corre, K.S., Valsami-Jones, E., Hobbs, P., and Parsons, S.A. (2009) Phosphorus recovery from wastewater by struvite crystallization: a review. *Crit Rev Environ Sci Technol* **39**: 433–477.

Li, Q., Csetenyi, L., and Gadd, G.M. (2014) Biomineralization of metal carbonates by *Neurospora crassa*. *Environ Sci Technol* **48**: 14409–14416.

Li, Z., Bai, T., Dai, L., Wang, F., Tao, J., Meng, S., *et al*. (2016) A study of organic acid production in contrasts between two phosphate solubilizing fungi: *Penicillium oxalicum* and *Aspergillus niger*. *Sci Rep* **6**: 25313.

Li, B., Boiarkina, I., Yu, W., Huang, H.M., Munir, T., Wang, G.Q., and Young, B.R. (2019) Phosphorus recovery through struvite crystallization: challenges for future design. *Sci Total Environ* **648**: 1244–1256.

Liang, X., and Gadd, G.M. (2017) Metal and metalloid biorecovery using fungi. *J Microbial Biotechnol* **10**: 1199–1205.

Liang, X., Hillier, S., Pendlowski, H., Gray, N., Ceci, A., and Gadd, G.M. (2015) Uranium phosphate biomineralization by fungi. *Environ Microbiol* **17**: 2064–2075.

Luo, Y., Li, H., Huang, Y.R., Zhao, T.L., Yao, Q.Z., Fu, S.Q., and Zhou, G.T. (2018) Bacterial mineralization of struvite using MgO as magnesium source and its potential for nutrient recovery. *Chem Eng J* **351**: 195–202.

Massey, M.S., Davis, J.G., Ippolito, J.A., and Sheffield, R.E. (2009) Effectiveness of recovered magnesium phosphates as fertilisers in neutral and slightly alkaline soils. *Agron J* **101**: 323–329.

Mastuli, M.S., Roshidah, R., Mahat, A.M., Saat, N., and Kamarulzaman, N. (2012) Sol-gel synthesis of highly stable nano sized MgO from magnesium oxalate dihydrate. *Adv Materials Res* **545**: 137–142.

Mayer, B.K., Baker, L.A., Boyer, T.H., Drechsel, P., Gifford, M., Hanjra, M.A., *et al*. (2016) Total value of phosphorus recovery. *Environ Sci Technol* **50**: 6606–6620.

Molinos-Senante, M., Hernández-Sancho, F., Sala-Garrido, R., and Garrido-Baserba, M. (2011) Economic feasibility study for phosphorus recovery processes. *Ambio* **40**: 408–416.

Priegnitz, B.E., Wargenau, A., Brandt, U., Rohde, M., Dietrich, S., Kwade, A., *et al*. (2012) The role of initial

spore adhesion in pellet and biofilm formation in *Aspergillus niger*. *Fungal Genet Biol* **49**: 30–38.
Prosser, J.I., and Tough, A.J. (1991) Growth mechanisms and growth-kinetics of filamentous microorganisms. *Crit Rev Biotechnol* **10**: 253–274.
Romani, A.M.P. (2013) Magnesium in health and disease. *Metal Ions Life Sci* **13**: 49–79.
Sayer, J.A., and Gadd, G.M. (1997) Solubilization and transformation of insoluble inorganic metal compounds to insoluble metal oxalates by *Aspergillus niger*. *Mycol Res* **101**: 653–661.
Sayer, J.A., and Gadd, G.M. (2001) Binding of cobalt and zinc by organic acids and culture filtrates of *Aspergillus niger* grown in the absence or presence of insoluble cobalt or zinc phosphate. *Mycol Res* **105**: 1261–1267.
Sayer, J.A., Raggett, S.L., and Gadd, G.M. (1995) Solubilization of insoluble metal compounds by soil fungi: development of a screening method for solubilizing ability and metal tolerance. *Mycol Res* **99**: 987–993.
Sayer, J.A., Kierans, M., and Gadd, G.M. (1997) Solubilization of some naturally-occurring metal-bearing minerals, limescale and lead phosphate by *Aspergillus niger*. *FEMS Microbiol Lett* **154**: 29–35.
Schugerl, K., Wittler, R., and Lorentz, T. (1983) The use of moulds in pellet form. *Trends Biotechnol* **1**: 120–122.
Sinha, A., Singh, A., Kumar, S., Khare, S.K., and Ramanan, A. (2014) Microbial mineralization of struvite: a promising process to overcome phosphate sequestering crisis. *Water Res* **54**: 33–43.
Soare, L.C., Bowen, P., Lemaitre, J., and Hofmann, H. (2006) Precipitation of nanostructured copper oxalate: substructure and growth mechanism. *J Phys Chem B* **110**: 17763–17771.
Talboys, P.J., Heppell, J., Roose, T., Healey, J.R., Jones, D. L., and Withers, P.J.A. (2016) Struvite: a slow-release fertiliser for sustainable phosphorus management? *Plant Soil* **401**: 109–123.
Tansel, B., Lunn, G., and Monje, O. (2018) Struvite formation and decomposition characteristics for ammonia and phosphorus recovery: a review of magnesium-ammonia-phosphate interactions. *Chemosphere* **194**: 504–514.
Tao, W., Fattah, K.P., and Huchzermeier, M.P. (2016) Struvite recovery from anaerobically digested dairy manure: a review of application potential and hindrances. *J Environ Manage* **169**: 46–57.
Tran, K.T., Van Luong, T., An, J.W., Kang, D.J., Kim, M.J., and Tran, T. (2013) Recovery of magnesium from Uyuni salar brine as high purity magnesium oxalate. *Hydrometallurgy* **138**: 93–99.
Tran, K.T., Han, K.S., Kim, S.J., Kim, M.J., and Tran, T. (2016) Recovery of magnesium from Uyuni salar brine as hydrated magnesium carbonate. *Hydrometallurgy* **160**: 106–114.
Vakilchap, F., Mousavi, S.M., and Shojaosadati, S.A. (2016) Role of *Aspergillus niger* in recovery enhancement of valuable metals from produced red mud in Bayer process. *Bioresour Technol* **218**: 991–998.
Veiter, L., Rajamanickam, V., and Herwig, C. (2018) The filamentous fungal pellet-relationship between morphology and productivity. *Appl Microbiol Biotechnol* **102**: 2997–3006.
Wargenau, A., and Kwade, A. (2010) Determination of adhesion between single *Aspergillus niger* spores in aqueous solutions using an atomic force microscope. *Langmuir* **26**: 11071–11076.
Wei, Z., Hillier, S., and Gadd, G.M. (2012) Biotransformation of manganese oxides by fungi: solubilization and production of manganese oxalate biominerals. *Environ Microbiol* **14**: 1744–1753.
Whitelaw, M.A. (2000) Growth promotion of plants inoculated with phosphate solubilizing fungi. *Adv Agron* **69**: 99–151.
Wittler, R., Baumgartl, H., Lubbers, D.W., and Schugerl, K. (1986) Investigation of oxygen transfer into *Penicillium chryogenum* pellets by microprobe measurement. *Biotechnol Bioeng* **28**: 1024–1026.
Xiao, C.-Q., Chi, R.-A., Huang, X.-H., Zhang, W.-X., Qiu, G.-Z., and Wang, D.-Z. (2008) Optimization for rock phosphate solubilization by phosphate-solubilizing fungi isolated from phosphate mines. *Ecol Eng* **33**: 187–193.
Zhang, J., and Zhang, J. (2016) The filamentous fungal pellet and forces driving its formation. *Crit Rev Biotechnol* **36**: 1066–1077.
Zhang, Y., Chen, F.S., Wu, X.Q., Luan, F.G., Zhang, L.P., Fang, X.M., *et al*. (2018) Isolation and characterization of two phosphate-solubilizing fungi from rhizosphere soil of moso bamboo and their functional capacities when exposed to different phosphorus sources and pH environments. *PLoS One* **13**: e0199625.
Zhao, T.L., Li, H., Huang, Y.R., Yao, Q., Huang, Y.Z., and Zhou, G.T. (2019) Microbial mineralization of struvite: salinity effect and its implication for phosphorus removal and recovery. *Chem Eng J* **358**: 1324–1331.